

https://doi.org/10.1070/QEL17578

Optical frequency standard with a single $^{171}Yb^{+}$ ion

S.V. Chepurov, N.A. Pavlov, A.A. Lugovoy, S.N. Bagayev, A.A. Taichenachev

Abstract. **We report recent results on the development of an optical frequency standard based on the quadrupole transition in a single $^{171}Yb^{+}$ ion. The probe laser frequency is simultaneously stabilised to the transmission peak of a Fabry–Perot reference cavity and the central resonance of the quadrupole transition of the ion with a linewidth of 30 Hz. With the experimentally obtained spectral characteristics of the probe laser and optical reference, a daily frequency stability on the order of 10^{-17} is demonstrated for the $^{171}Yb^{+}$ standard.**

Keywords: *quadrupole trap, laser cooling, spectroscopy, frequency stabilisation, optical frequency standard.*

1. Introduction

The urgency of the research and developments aimed at designing optical frequency standards with a long-term stability no worse than 10^{-17} is due to the extraordinary high demand for these standards in modern science (verification of fundamental physical theories, testing of the hypothetical drift of fundamental constants, justification of cosmological models, etc. [1–3]), as well as their wide practical application (plotting of exact maps of orthometric heights, navigation in physical fields, detection of geological voids and deposits of mineral resources, etc. [4–6]). In addition, significant progress in the frequency measurement methods opens a possibility of improving essentially the accuracy of determining other physical values allowing for conversion into frequency measurements (for example, gravitational potential, magnetic field, electric field, etc.). Practical implementation of the above-stated purposes opens new prospects in information technologies, physical measurements, and life sciences.

In the last decade, great progress has been made in improving the stability and accuracy of optical frequency standards using atoms and ions that are spatially localised and cooled to ultralow temperatures. Currently, these systems demonstrate the best frequency stability (to 10^{-18}) for long observation times [7–9]. The key advantage of these standards is that the atom or ion with a forbidden ultranarrow transition (used as an optical frequency standard) in the energy-level structure is in a well-controlled environment, isolated to a great extent from external effects.

In this paper, we report the results of the studies performed at the Institute of Laser Physics of the Siberian Branch of the Russian Academy of Sciences (ILP SB RAS) that were aimed at developing an optical frequency standard based on the quadrupole transition in a single ^{171}Yb ion, with a relative uncertainty and long-term frequency instability less than 10^{-17}.

2. Ion trapping and cooling

Figure 1 shows a schematic of the optical frequency standard with a single ^{171}Yb ion, developed at the ILP SB RAS. The ion trapping and confinement are performed by a miniature RF Paul trap with endcap electrodes [10, 11]. An ac voltage with an amplitude of 600 V and a frequency of 14 MHz is used to form a 3D confining potential. The potential-well depth is 18 eV, and the trap secular frequencies are $\nu_z = 2\nu_r = 1.2$ MHz. To increase the ion localisation time, the trap is placed in a vacuum chamber with a residual gas pressure less than 5×10^{-10} Torr, due to which the ion loss caused by collisions with gas molecules can be minimised.

Doppler cooling and detection of ion state are performed using frequency-modulated radiation of a diode laser with a wavelength $\lambda = 369.5$ nm [12, 13]. Modulation is carried out by an electro-optic modulator (EOM) at a frequency of 14.75 GHz in order to generate the spectral component exciting the hyperfine component of the cooling transition $^2S_{1/2}$ $(F = 0) \rightarrow {}^2P_{1/2}$ $(F = 1)$, which is not excited by the resonance cooling radiation. The $^2D_{3/2}$ and $^2F_{7/2}$ levels are depopulated using radiation of pump diode lasers with wavelengths of 935 and 760 nm, respectively.

The ion fluorescence, induced by the cooling laser, is projected (using a multilens objective) onto a photoelectron multiplier tube (PMT) and a CCD camera. The camera image is used to determine the number of trapped particles and monitor the ion position in the trap. The PMT signal serves to determine the total fluorescence rate with a high temporal resolution.

Figure 2 shows an image of a single ^{171}Yb ion in the RF trap and the resonance fluorescence signal on the cooling transition. The signal full width at half maximum (FWHM) is ~20 MHz, which indicates the absence of Doppler broadening and, therefore, demonstrates efficient ion cooling.

3. Minimisation of ion excess micromotion

An ion localised in a trap, being displaced from the region of the zero confinement potential, may be affected by the ac RF electric field. The field-induced vibrational motion of the ion

S.V. Chepurov, N.A. Pavlov, A.A. Lugovoy, S.N. Bagayev, A.A. Taichenachev Institute of Laser Physics, Siberian Branch, Russian Academy of Sciences, prosp. Akad. Lavrent'eva 13/3, Novosibirsk, 630090 Russia; e-mail: svc972@gmail.com

Received 16 March 2021
Kvantovaya Elektronika **51** (6) 473–478 (2021)
Translated by Yu.P. Sin'kov

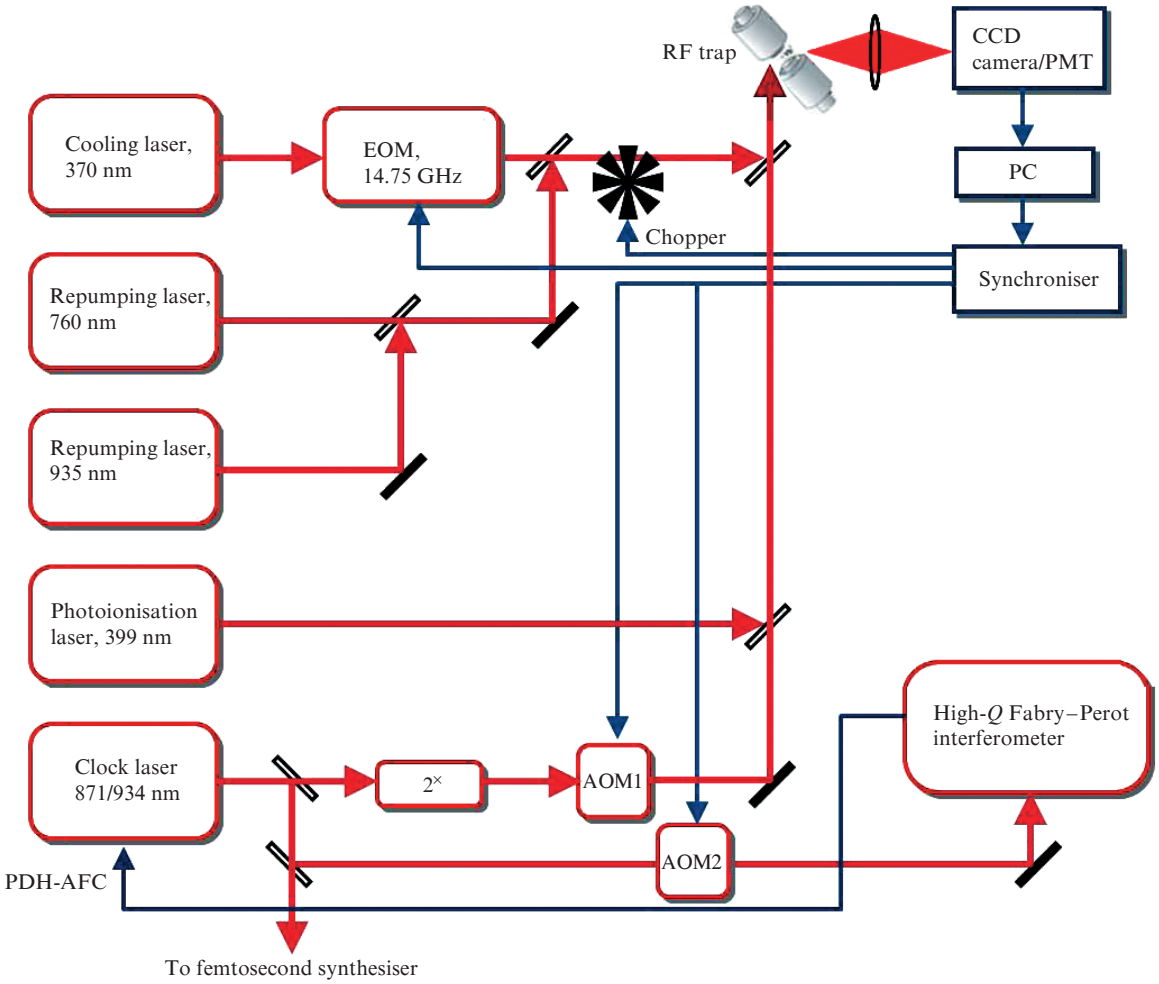

Figure 1. Schematic of the optical frequency standard with a single ytterbium ion.

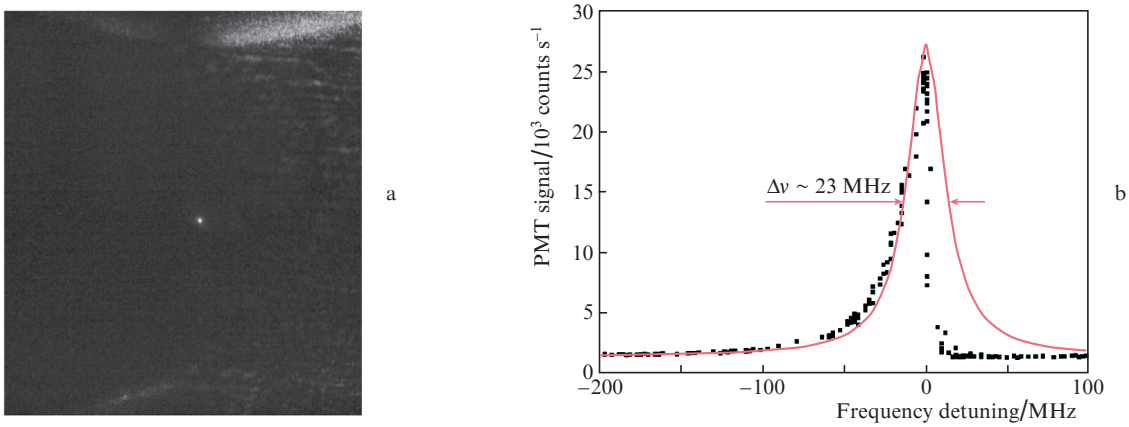

Figure 2. (a) Image of a trapped single ^{171}Yb ion and (b) a resonance fluorescence signal from a cooled single ion, obtained by scanning cooling laser frequency. The solid line is the Lorentzian approximation of spectral line.

at the field frequency (the so-called micromotion) leads to an increase in its temperature and spectral broadening of the clock transition due to the Doppler effect. The ion displacement from the trap centre is mainly due to the action of uncompensated spurious static electric fields.

In this study, to detect and compensate for the ion excess micromotion in a trap, we applied the cross-correlation method [14], in which the ion fluorescence modulation related to the first-order Doppler shift correlates with the phase of the electric field formed by the trap electrodes.

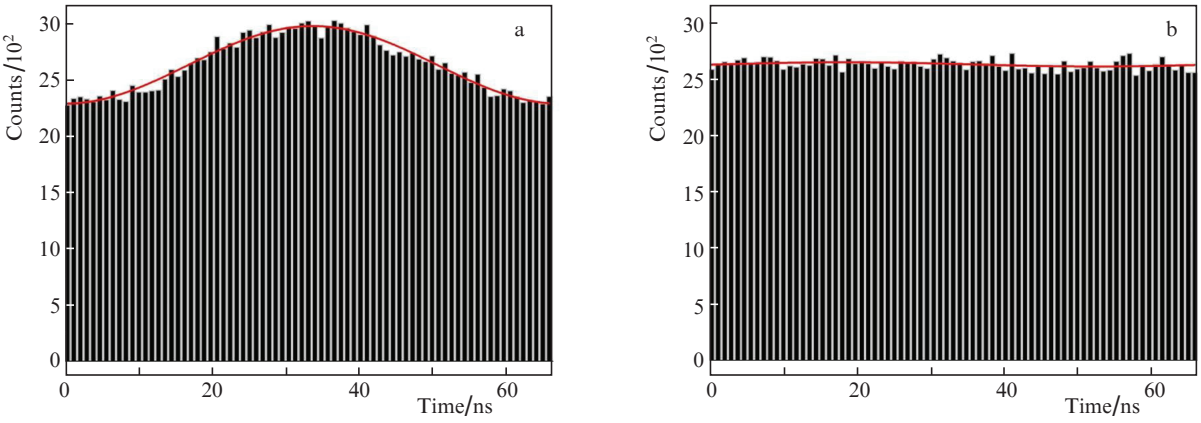

Figure 3. Cross-correlation signals (a) at ion displacement with respect to the trap centre (in the presence of uncompensated spurious fields) and (b) after correcting the ion position (with fields compensated). Approximation by a sine function.

The cross-correlation signal is obtained using a counter, for which the starting pulse is the PMT signal, generated when recording a photon from the ion fluorescing in the cooling cycle. The count is stopped when the sinusoidal signal of the electric field crosses '0' in the negative direction. Then the number of photons arrived for the certain time of change in the trap field phase is counted.

Figure 3 shows the cross-correlation signals for an ion displaced from the trap centre, before and after correcting its position by applying a dc voltage to the compensation electrodes. The error in compensating for the ion displacement by this method turned out to be ~15 nm, which is smaller than the Lamb–Dicke parameter ($d < \lambda/\pi \approx 118$ nm) and sufficient to minimise the Doppler effect. Important advantages of this method for detecting and compensating for ion displacements in a trap according to the conventional technique with application of highly sensitive (and expensive) CCD cameras are the higher sensitivity and accuracy of positioning. In addition, the use of noncoplanar cooling beams, having nonzero projections on all trap axes, allows one to detect and compensate for the ion micromotion in all coordinates.

4. Detection of quadrupole transition

The quadrupole clock transition $^2S_{1/2}$ ($F = 0$) → $^2D_{3/2}$ ($F = 2$) is excited by the second-harmonic radiation of an external-cavity diode (clock) laser at a wavelength of 871 nm [11]. To reduce the spectral linewidth of the laser to ~1 Hz, its frequency is stabilised to a Fabry–Perot reference cavity, made of glass with a low thermal-expansion coefficient (ULE glass, Corning). To suppress mechanical vibrations, the vacuum chamber with the cavity was installed on a passive vibration-isolation plate. In addition, the cavity was mounted in the chamber using a system of suspensions, reducing its sensitivity to vibrations [15]. The influence of the ambient temperature on the position of cavity resonances was significantly reduced by stabilising temperature near the 'zero' point, characterised by close-to-zero thermal-expansion coefficient of the cavity base material.

The principle of observation of resonances in single ions is based on the method of detecting a quantum jump (transition of the ion from one energy state to another) by fixing the onset of fluorescence on the cooling transition (electron shelving [16–18]). The preparation and inquiry of ion energy states are performed using a specially chosen sequence of laser pulses [11]. If the fluorescence signal is absent for some time (several milliseconds in the case of the quadrupole transition) after switching off the probe laser and switching on the cooling cycle, the ion exists with a high probability in the excited state $^2D_{3/2}$, and the excitation cycle is considered as successful. The sequence of cooling, excitation, and detection cycles is repeated several times for one probe laser frequency, and the probability of exciting the $^2D_{3/2}$ level ($F = 2$, $m_F = 0$) is recorded as a frequency function. The detected excitation spectrum of the quadrupole transition consists of several resonances, which contain information about the state of the ion, its motion in the trap, and its interaction with the environment.

Figure 4 shows the results of detecting the excitation spectrum of the quadrupole transition $^2S_{1/2}$ ($F = 0$) → $^2D_{3/2}$ ($F = 2$) in the ^{171}Yb ion [11]. The spectrum of the magnetic sublevels of the transition (Fig. 4a) consists of five components, corresponding to $\Delta m_F = 0$, ±1, and ±2. It can be seen that the magnetic splitting of the sublevels is ~50 kHz, which corresponds to a residual magnetic field $|B| \approx 6$ μT in the trap. The spectrum of the central component $\Delta m_F = 0$ of the quadrupole transition is shown in Fig. 4b. In this case, a 30-ms pulse of the clock laser was used to excite the resonance. The FWHM value for the recorded resonance on the transition central frequency is about 30 Hz at an excitation probability of ~0.5.

5. Stabilisation of the probe laser frequency to the quadrupole transition frequency

A high short-term stability of the standard frequency is attained by stabilising the frequency of the diffracted beam of the probe clock laser at the output of acousto-optic modulator AOM1 (see Fig. 1) to the reflection resonances of a high-Q Fabry–Perot interferometer by the Pound–Drever–Hall (PDH) method using an automatic frequency control (PDH-AFC) system. The long-term stability of the system is obtained by tuning the AOM1 frequency so as to make the frequency of the probe laser second harmonic coincide with the frequency corresponding to the maximum of excitation probability signal for the clock transition in the RF-trapped single ion. A digital AFC system (based on a computer) corrects the AOM1 frequency for characteristic times providing the corresponding signal-to-noise ratio to achieve the desired stability (in the case of single ions, the characteristic times are gen-

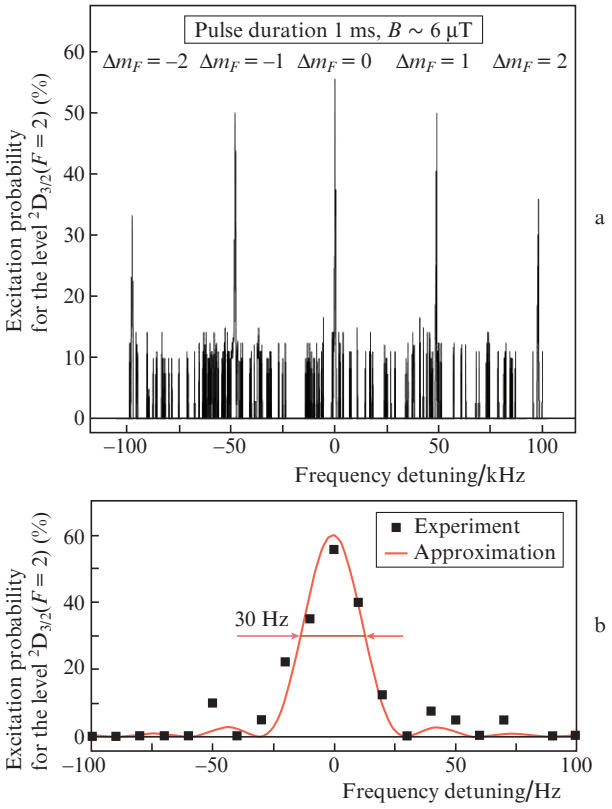

Figure 4. Excitation spectra of the quadrupole transition $^2S_{1/2}$ ($F = 0$) → $^2D_{3/2}$ ($F = 2$) in the ^{171}Yb ion: (a) spectrum of the magnetic sublevels of the transition and (b) spectrum of the central component $\Delta m_F = 0$ at probe frequency scan rates of (a) 500 and (b) 10 Hz s^{-1}.

erally no shorter than 100 s). The error signal for determining the position of the probe-laser second-harmonic frequency relative to the transition centre is the difference in the excitation probability at detunings to both sides from the resonance centre by its halfwidth, which are implemented by tuning the probe frequency using an AOM2. Thus, the standard frequency stability for short times (less than 100 s) is determined by the properties of the Fabry–Perot interferometer, whereas the characteristics of the long-term stability and accuracy of the standard are determined by the parameters of the resonance on the ultranarrow (forbidden in the dipole approximation) optical transition.

In accordance with the above-described technique we performed simultaneous stabilisation of the probe laser frequency to the transmission peak of the Fabry–Perot reference cavity and the central-resonance frequency of the Yb-ion quadrupole transition.

Before stabilising the laser frequency to the atomic-transition resonance frequency ν_0, the resonance excitation spectrum is recorded, and the laser frequency is set to be close to the resonance centre. In the resonance recording regime the laser frequency is tuned discretely relative to the reference interferometer mode. The initial detuning, the final detuning, the detuning step, and the direction of frequency change are set in the dialogue window of the specially developed experiment control program. In addition, the choice of the generator resonance, controlled during recording, makes it possible to choose an AOM providing necessary probe frequency tuning. When recording the resonance, the fluorescence signal from PMT is synchronised with the signals forming a temporal sequence of clock transition excitation and detection events. After tuning the probe frequency, several (generally, 10–20) elementary inquiry cycles are performed, which give as a result either 0 or 1. Another possible version is the exclusion of the result of a given or next cycle from consideration ('poor' cycle). To this end, in each ~100-ms-long cycle, the correspondence of the fluorescence signal from PMT in specified time intervals (determined by the time sequence of clock transition excitation and detection) to the user-specified criteria is verified, on the basis of which one determines is the performed inquiry cycle should be considered as 'reliable' or 'poor'. If the cycle is 'reliable', one determines if the ion excitation from the ground state occurred or not. The number of 'successful' cycles at a given detuning is increased by unity if the transition occurred and by zero in the opposite case.

After finishing data collection at a given detuning, the probability of ion excitation is calculated as the ratio of the number of 'successful' cycles to the number of 'reliable' cycles. The ratio of the number of 'successful' inquiries to the total number of performed cycles can also be considered as a result; however, because of the inevitable presence of 'poor' cycles, the maximum attainable probability is lower in this case.

Many methods have been developed to stabilise laser frequency using digital algorithms (see, for example, [19]). For the symmetric resonance, observed on transitions in single particles, the simplest is the two-point stabilisation technique, where the role of frequency discriminator is played by the difference in the resonance amplitudes at equal detunings on the left and on the right from the resonance centre; i.e., the discriminator slope is $k = (A_+ - A_-)/\delta$, where A_+ and A_- are the values of recorded signal at positive and negative detunings δ, respectively. The recorded signal is the quadrupole transition excitation probability, which is detected when carrying out a specified number of above-described elementary cycles of ion inquiry. After determining the quadrupole transition excitation probability at specified positive and negative detunings (P_+ and P_-) with allowance for the specified resonance slope, the current detuning of the laser frequency from the resonance centre, $\Delta = (P_+ - P_-)/k$, is calculated. A standard PI controller in the form of $u = \mathrm{P} + \mathrm{I}$, where $\mathrm{P} = k_\mathrm{P}\Delta$ and $\mathrm{I} = k_\mathrm{I}\Sigma\Delta$, is used to form a stable digital feedback circuit. The factors related to the proportional (k_P) and integral (k_I) units of the PI controller, along with the detuning δ and discriminator slope k, are set in the dialogue window of the control program. The dynamics of the PI controller functioning is optimised during stabilisation by fitting the factors k_P and k_I, proceeding from the criterion of minimising the temporal fluctuations of stabilised-laser frequency.

6. Estimation of optical standard frequency instability

The instability of frequency is determined by the degree of its deviation from the nominal value for the measurement time. The most widespread criterion of instability for frequency standards is the Allan variance $\sigma_y^2(\tau)$. However, the Allan parameter (or deviation) $\sigma_y(\tau)$ is often used in practice. For a set of frequency values N, with a duration τ of each measurement, the Allan parameter can be written as

$$\sigma_y(\tau) = \left[\frac{1}{2(N-1)}\sum_{n=1}^{N-1}(y_{n+1} - y_n)^2\right]^{1/2}, \qquad (1)$$

where y_n is the average beat frequency (difference of laser frequencies) for the averaging time τ, divided by the nominal frequency, n is the measurement number, and N is the total number of measurements.

To characterise the frequency properties of the $^{171}Yb^+$ standard, we measured the frequency instabilities for the beat signal of probe laser frequency at $\lambda = 871$ nm and the component of emission spectrum frequency of femtosecond generator Menlo Systems FC1500-250-WG, stabilised to the frequency of the Yb:YAG/I_2 standard. The beat frequency instability was determined as the Allan parameter (1). The measurement results are presented in Fig. 5. The values of the Allan parameter for averaging times $\tau < 100$ s are determined by the frequency characteristics of the Yb:YAG/I_2 standard [20]; furthermore, when the system of stabilisation of the probe laser frequency to the optical reference is switched on, they decrease according to $\propto \tau^{-1/2}$. The Allan parameter for the beat signal was measured to be $\sim 3 \times 10^{-15}$ at an integration time of 10^3 s.

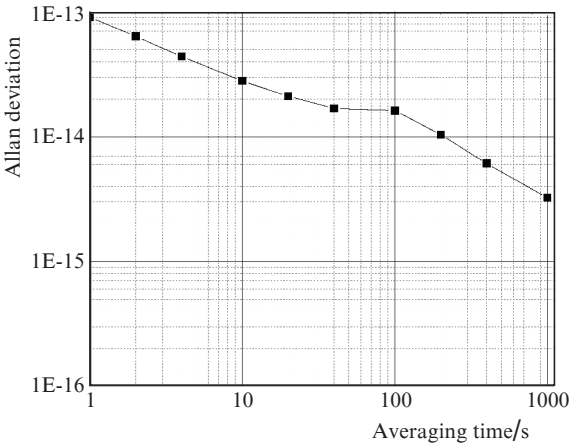

Figure 5. Allan deviation for the beat signal of the clock laser frequency and the spectral component of a femtosecond generator stabilised to the frequency of Yb:YAG/I_2 standard.

The most correct estimation of frequency standard stability is obtained when comparing two identical systems. Currently, the second standard on $^{171}Yb^+$ ion is being developed at the ILP SB RAS. To estimate the long-term stability of the $^{171}Yb^+$ standard, we modelled the Allan parameter based on the obtained experimental values of the linewidth and drift rate of probe laser frequency, resonance width, and quadrupole transition excitation probability (Fig. 6).

To analyse the frequency instability in the case of a single ion, where the main noise source is the quantum projection noise, it is pertinent to use the model implying single-pulse excitation and inquiry of resonances (Rabi excitation) [21]. In this case, the Allan parameter is reduced to the form

$$\sigma_y(\tau) = S_p \frac{1}{2\pi\nu_0\tau_0}\sqrt{\frac{\tau_0}{\tau}}. \qquad (2)$$

Here,

$$S_p = \sqrt{\tfrac{1}{2}p_{\max}\left(1 - \tfrac{1}{2}p_{\max}\right)}\,\frac{\Delta\omega_0\tau_0}{p_{\max}}\sqrt{\frac{t + t_d}{\tau_0}} \qquad (3)$$

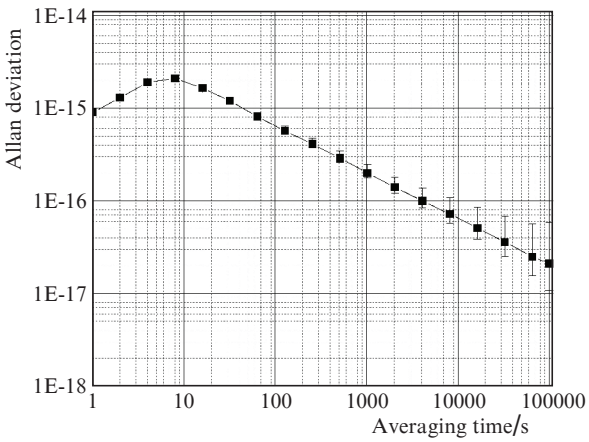

Figure 6. Estimation of the long-term stability of $^{171}Yb^+$ standard based on the experimentally obtained spectral characteristics of probe laser and optical reference.

is the dimensionless stability parameter. The profile FWHM $\Delta\omega_0$ is determined by the resonance detuning at which the central resonance excitation probability $p_{\max}$ decreases to $p_{\max}/2$. The first factor in (3) describes the quantum fluctuations (projection noise) at the detuning frequency to a half linewidth, and the second factor is inversely proportional to the error signal slope. The last factor describes the time t_c spent on one excitation cycle; $t_c = t + t_d$, where t is the probe time and t_d is the 'dead' time, which is necessary for determining the ion state, laser cooling, and preparing the next inquiry cycle. The excited state lifetime τ_0 is a scaling parameter for time and frequency.

The following data were used to calculate the Allan deviation (2): the central resonance frequency of the quadrupole transition, $\nu_0 =$ = 688.358974 THz; the excited state lifetime $\tau_0 = 1/(2\pi\nu_0) = 50$ ms; the central resonance excitation probability $p_{\max} = 0.5$; the FWHM value for the central resonance, $\Delta\omega_0/2\pi = 30$ Hz; the probe pulse width $t = 30$ ms; the excitation cycle duration $t_c = 100$ ms; and the probe frequency linear drift equal to 0.04 Hz/s.

The short-term instability of a frequency standard is mainly determined by the linewidth of the probe laser, stabilised to the reference cavity. As a result of the probe frequency drift, the quantity $\sigma_y(y)$ becomes maximum at $\tau \approx 80t_c$ (or $\tau \approx 1.5t_{servo}$) and then, after switching on the system of laser frequency stabilisation to resonance, decreases as $\tau^{-1/2}$ for $\tau > 100t_c$ (Fig. 6). With correctly chosen feedback loop coefficients, the long-term stability is mainly limited by quantum fluctuations and is independent of the laser frequency noise [21]. With allowance for the observed dependence $\sigma_y(\tau) \sim \tau^{-1/2}$, the daily frequency stability of the developed frequency standard was estimated to be $\sim 10^{-17}$ (see Fig. 6).

7. Conclusions

In this paper, we have reported the results of current studies aimed at developing an optical frequency standard based on the quadrupole transition of a single ^{171}Yb ion.

The ion trapping and confinement are performed using a miniature RF trap with endcap electrodes. Laser cooling of the ion and detection of its state are implemented on the quasicyclic dipole transition with a wavelength of 370 nm. The quadrupole transition is excited by a narrowband probe laser with

$\lambda = 436$ nm. The preparation and inquiry of ion energy states are performed using a specially chosen sequence of laser pulses. The width of the recorded resonance at the central transition frequency is 30 Hz.

Simultaneous stabilisation of the probe laser frequency to the transmission peak of the Fabry–Perot reference cavity and the central resonance frequency of the quadrupole transition of ytterbium ion was performed.

The frequency instability of the beat signal of the probe laser frequency at $\lambda = 871$ nm and the spectral component of the femtosecond generator, stabilised to the frequency of the $Yb:YAG/I_2$ standard, was measured to characterise the frequency properties of the $^{171}Yb^+$ standard. The Allan parameter for the beat signal was measured to be $\sim 3 \times 10^{-15}$ at an integration time of 10^3 s.

To estimate the long-term stability of the $^{171}Yb^+$ standard, we modelled the Allan parameter based on the obtained experimental values of the linewidth and drift rate of the probe laser frequency, resonance width, and quadrupole transition excitation probability. The daily frequency stability of the developed standard was estimated to be $\sim 10^{-17}$.

Acknowledgements. We are grateful to M.N. Skvortsov and S.M. Ignatovich for supplying the $Yb:YAG/I_2$ standard.

This work was supported by the Russian Foundation for Basic Research (Grant No. 20-32-90135).

References

1. Godun R.M. et al. *Phys. Rev. Lett*., **113** (21), 210801 (2014).
2. Huntemann N. et al. *Phys. Rev. Lett*., **113** (21), 210802 (2014).
3. Joao S.M. et al. *Phys. Lett. B*, **749**, 389 (2015).
4. Vutha A. *New J. Phys*., **17**, 6 (2015).
5. Chou C.W. et al. *Science*, **329** (5999), 1630 (2010).
6. Bondarescu R. et al. *Geophys. J. Int*., **202** (3), 1770 (2015).
7. Huntemann N. et al. *Phys. Rev. Lett*., **116**, 063001 (2016).
8. Cao J. et al. *Appl. Phys. B*, **123** (4), 1 (2017).
9. Brewer S.M. et al. *Phys. Rev. Lett*., **123**, 033201 (2019).
10. Schrama et al. *Opt. Commun*., **101**, 32 (1993).
11. Chepurov S.V. et al. *Quantum Electron*., **49** (5), 4127 (2019) [*Kvantovaya Elektron*., **49** (5), 4127 (2019)].
12. Chepurov S.V. et al. *Quantum Electron*., **44** (6), 527 (2014) [*Kvantovaya Elektron*., **44** (6), 527 (2014)].
13. Prudnikov O.N. et al. *Quantum Electron*., **47** (9), 806 (2017) [*Kvantovaya Elektron*., **47** (9), 806 (2017)].
14. Berkeland D.J. et al. *J. Appl. Phys*., **83** (10), 5025 (1998).
15. Nazarova T. et al. *Appl. Phys. B*, **83**, 531 (2006).
16. Nagourney W., Sandberg J., Dehmelt H. *Phys. Rev. Lett*., **56** (26), 2797 (1986).
17. Buhner V., Tamm Chr. *Phys. Rev. A*, **61**, 061801 (2000).
18. Dehmelt H. *IEEE Trans. Instrum. Meas*., **31**, 83 (1982).
19. Bagaev S.N. et al. *Quantum Electron*., **38** (1), 59 (2008) [*Kvantovaya Elektron*., **38** (1), 59 (2008)].
20. Ignatovich S.M. et al. *IOP Conf. Ser.: J. Phys.: Conf. Ser*., **793**, 012010 (2017).
21. Peik E., Schneider T., Tamm Chr. *J. Phys. B: At. Mol. Opt. Phys*., **39**, 145 (2006).